Modelling by Homogenization of the Long-Term Rock Dissolution and Geomechanical Effects

Jolanta Lewandowska

Modelling by homogenization of the long term rock dissolution and geomechanical effects

Jolanta Lewandowska
University of Montpellier 2, Laboratory of Mechanics and Civil Engineering LMGC

1. Introduction

The geological storage of CO_2 coming from large industrial facilities has been studied in detail for the last several years as a solution against the greenhouse effect and climate change in a number of countries. It is considered as a complementary solution together with the research for the non pollutant or/and renewable energy sources. One of the available options is the injection of the supercritical CO_2 in the saline aquifers. The idea of geological storage resides in various mechanisms of trapping coming into play progressively over time. In the short term the migration of CO_2 is principally blocked by the impervious rock lying on the top of the aquifer. As time goes on, other mechanisms appear, in particular of geochemical nature, like the dissolution of CO_2 in pore water, and finally the chemical reactions resulting in dissolution and /or precipitation of rock minerals. These reactions can generate important and irreversible modifications of the hydrodynamical as well as geomechanical properties of the reservoir.

The long-term safety of the CO_2 storage sites requires the understanding of the physicochemical processes related to the injection of the CO_2 in the geological medium and their consequences, especially for the stability of the reservoir. These processes are still not completely known, in particular because of the complexity of natural systems, those are very often heterogeneous and multiscale, and also because of multiphysical couplings engendered by the CO_2 injection.

The experimental studies of CO_2 injection into rock samples, conducted in the laboratory conditions, show different behaviour depending on the injection rate, the composition of the injected fluids and the nature of the rock (e.g. [LUQ 09, GOU 10, EGE 05, IZG 08]) The investigations focused on the long term behaviour assume that the rock is saturated with an acidified aqueous CO2 solution, and homogeneous chemical alteration occurs. The results of experimental studies conducted in such conditions show global porosity increase homogeneously distributed over the sample length (e.g. [NGU 11, BER 09]). Moreover, it was observed that chemical alteration induces mechanical weakening of the rocks with a decrease of both stiffness and shear strength. The triaxial testing in drained conditions on the altered carbonate samples showed the decrease of the elastic bulk modulus and the shear modulus (e.g. [NGU 11, BER 09]). Although this behaviour has been reported in the literature, very few contributions concerning the modelling of long term geomechanical effects related to CO_2 storage are proposed. Of special interest in this case are the micromechanical methods because they provide suitable mathematical framework, capable to produce multiscale and multiphysics models of high predictive capacity.

2. Microstructure and modelling by homogenization.

Let us assume that the microstructure of the porous rock is known, Figure 1. We consider a porous medium with two phases: solid skeleton and (saline) water saturating the pores. Both

phases are assumed to be connected. The water contains the dissolved CO_2. The porous medium is periodic and the periodic volume is representative from the point of view of both the microstructure and the phenomena taking place at the microscopic scale. We assume that the conditions of scale separation are satisfied, which means that the size of the period (l) is very small with respect to the dimension of the aquifer (L). Mathematically, this condition is written in the form:

$$\varepsilon = \frac{\ell}{L} << 1 \qquad [1]$$

where ε is the small parameter of homogenization.

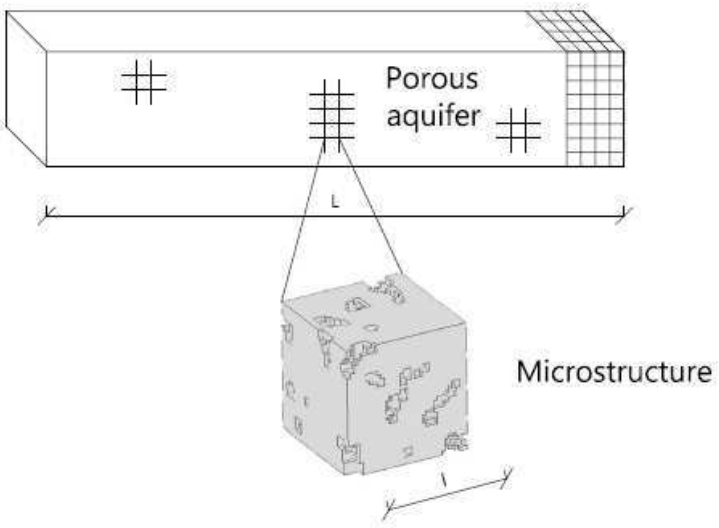

Figure 1. The porous aquifer with the microstructure

The following phenomena will be taken into account:

- The water flow through the pores (named hydraulic “H-problem”)
- The solid deformation (named mechanical “M-problem”)
- The transport of dissolved CO_2 (named transport “T-problem”)
- The chemical dissolution of solid (named chemical “C-problem”)

The aim of the analysis is to develop of a macroscopic model of the behaviour of the system by using the method of homogenization of periodic structures ([SAN 80, BEN 78]). The analysis will be presented in two stages. In the first stage (section 3) the homogenization of the problem of water flow, solid deformation and CO_2 transport (the “H-M-T problem”), will be analysed. We will use the principal results of homogenization of the “H-M problem” and the “T problem” that were previously analyzed as uncoupled problems ([AUR 77, AUR 96]). In the second stage (section 4), the chemo-mechanical coupling will be considered (the “C-M problem”). At this stage it will be assumed that the whole aquifer is subjected to homogeneous solid dissolution caused by chemical reaction between solid components and

acid pore water. We will focus on the modification of the microstructure of the porous aquifer and progressive decrease of the mechanical parameters. In section 5 numerical computations of the chemo-mechanical coupling and the chemical degradation of the rock mechanical parameters will be presented.

3. Homogenization of the H-M-T problem

In order to model the coupled H-M-T behaviour at the macroscopic scale, the differential equations are firstly formulated at the microscopic (pore) scale. This formulation concerns: the equilibrium equation for stresses in the solid phase, the momentum equation for fluid flow, the mass balance equation of concentration of the dissolved CO_2, and the appropriate interface conditions. Then, the classical homogenization process by using the asymptotic developments method ([SAN 80, BEN 78]), is carried out.

3.1 Formulation of the problem at the microscopic scale

The assumptions are as follows:

- The porous medium is saturated by viscous incompressible fluid (eg. saline water)
- The fluid is saturated by the dissolved CO_2
- The fluid flow is slow and laminar
- The transport of the CO_2 dissolved in fluid is governed by convection and diffusion mechanism
- Small displacements and deformations of the solid
- Linear elastic constitutive law for solid material
- Quasi static deformation process

The following set of differential equations can be written in the domain of the period (Fig. 2):

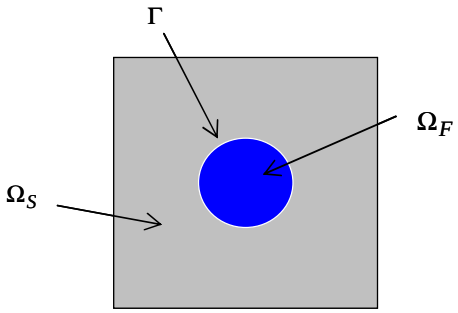

Figure 2. The period of the porous medium

Stress equilibrium of the solid phase:

$$\frac{\partial \sigma_{Sij}}{\partial X_j} = 0 \ in \ \Omega_S \qquad [2]$$

$$\sigma_{Sij} = a_{ijkl}\, e_{kl}(\boldsymbol{u}) \qquad [3]$$

with $e_{kl} = 1/2\,(u_{k,l} + u_{l,k})$

- Stress equilibrium and incompressibility condition of the fluid phase:

$$\frac{\partial \sigma_{Fij}}{\partial X_j} = 0 \ in \ \Omega_F \qquad [4]$$

$$\sigma_{Fij} = - p\delta_{ij} + \mu_F (v_{i,j} + v_{j,i}) \ in \ \Omega_F \qquad [5]$$

$$\frac{\partial v_i}{\partial X_i} = 0 \ in \ \Omega_F \qquad [6]$$

- Mass balance equation of the CO_2 dissolved in the fluid phase:

$$\frac{\partial c}{\partial t} + \frac{\partial}{\partial X_i}(-D_{ij} \frac{\partial c}{\partial X_j} + v_i c) = 0 \ in \ \Omega_F \qquad [7]$$

- Continuity conditions at the solid-fluid interface:

$$\sigma_{Sij} N_j - \sigma_{Fij} N_j = 0 \ in \ \Gamma \qquad [8]$$

$$\dot{u}_i - v_i = 0 \ on \ \Gamma \qquad [9]$$

- Zero-flux condition at the solid-fluid interface:

$$(-D_{ij} \frac{\partial c}{\partial X_j}) N_i = 0 \ on \ \Gamma \qquad [10]$$

where : $_S$ is the stress tensor in the solid, $_F$ is the stress tensor in the fluid, $\boldsymbol{a}$ is the microscopic rigidity tensor of the solid, $\boldsymbol{e}$ is the small deformation tensor in the solid, $\boldsymbol{u}$ is the displacement vector in the solid, p is the water pressure, μ_F is the viscosity of the fluid, c is the concentration of the CO_2 dissolved in water, $\boldsymbol{D}$ is the diffusion tensor of the CO_2 in water, $\boldsymbol{v}$ is the water flow velocity, **N** is the unit normal outward vector.

Before starting the homogenization, the description [2]–[10] has to be rewritten using the non-dimensional variables. We adopt here the so called “microscopic point of view” [AUR 91] which means that the length scale used in the normalization will be the microscopic dimension l. For the physical (dimensional) space variable $\boldsymbol{X}$ two non-dimensional space variables are defined:

$$\boldsymbol{x} = \frac{\boldsymbol{X}}{L} \text{ and } \boldsymbol{y} = \frac{\boldsymbol{X}}{\ell}$$

The homogenization problem will be analyzed at two scales $\boldsymbol{x}$ and $\boldsymbol{y}$ simultaneously.

The introduction of the non-dimensional variables is related with the evaluation of the order of magnitude of several quantities appearing in the microscopic model [2]–[10]. As a unit of

measure in this evaluation, the powers of the small parameter ε are used. The following estimations are supposed valid:

- The Reynolds number is: $\mathrm{Re}_l = \dfrac{\rho\, v\ell}{\mu_F} = O(\varepsilon^1)$ where ρ is the volumetric density of the fluid.
- The macroscopic gradient of water pressure is of the same order of magnitude as the microscopic viscous term: $p / L = O(\mu_F\, v / \ell^2)$.
- The local Péclet number is such that there is no dispersion: $Pe_l = \dfrac{v\ell}{D} = O(\varepsilon^1)$
- The time scale t_c corresponds to the mass transport by diffusion at the macroscopic scale L, thus the associated non-dimensional number is $P_l = \dfrac{\ell^2}{D\, t_c} = O(\varepsilon^2)$
- The displacements and stresses in solid and in fluid are of the same orders of magnitude: $u_{Si} = O(u_{Fi})$ and $\sigma_{Sij} = O(\sigma_{Fij})$

More details concerning the evaluations of the orders of magnitude can be found in ([AUR 91], [AUR 77], [AUR 96]). Finally, the non-dimensional description takes the following form:

$$\frac{\partial}{\partial y_j}(a_{ijkl}\, e_{ykl}(\boldsymbol{u})) = 0 \ in\ \Omega_S \qquad [11]$$

$$\varepsilon\, \mu_F \frac{\partial^2 v_i}{\partial y_j\, \partial y_j} - \frac{\partial p}{\partial y_i} = 0 \ in\ \Omega_F \qquad [12]$$

$$\frac{\partial v_i}{\partial y_i} = 0 \ in\ \Omega_F \qquad [13]$$

$$\varepsilon^2 \frac{\partial c}{\partial t} + \frac{\partial}{\partial y_{\mathrm{i}}}(-D_{ij} \frac{\partial c}{\partial y_{\mathrm{j}}} + v_i c) = 0 \ in\ \Omega_F \qquad [14]$$

The interface conditions are rewritten in the non-dimensional form:

$$(a_{\mathrm{ijkl}}\, e_{\mathrm{kl}}(\boldsymbol{u}) + p\delta_{ij} - \varepsilon\, \mu_F (v_{i,j} + v_{j,i}))N_j = 0 \ on\ \Gamma \qquad [15]$$

$$\dot{u}_i - v_{\mathrm{i}} = 0 \ on\ \Gamma \qquad [16]$$

$$(-D_{ij} \frac{\partial c}{\partial X_{\mathrm{j}}})N_i = 0 \ on\ \Gamma \qquad [17]$$

The interface conditions [15]- [17] are completed by the periodicity conditions on the external boundaries of the period.

Note that for convenience we keep the same notations for the non-dimensional variables in [11]-[17] as for the dimensional variables in [2]-[10]. Further, we introduce the relative velocity $w_i = v_i - \dot{u}_i$ which is the velocity of the fluid with respect to the solid. Using the new definition of fluid velocity the problem can be rewritten in the form

$$\frac{\partial}{\partial y_j}(a_{ijkl}\, e_{ykl}(\boldsymbol{u})) = 0 \ in\ \Omega_S \qquad [18]$$

$$\varepsilon\,\mu_F \frac{\partial^2 w_i}{\partial y_j\,\partial y_j} - \frac{\partial p}{\partial y_i} = 0 \ in\ \Omega_F \qquad [19]$$

$$\frac{\partial w_i}{\partial y_i} = 0 \ in\ \Omega_F \qquad [20]$$

$$\varepsilon^2 \frac{\partial c}{\partial t} + \frac{\partial}{\partial y_{\mathrm{i}}}(-D_{ij} \frac{\partial c}{\partial y_{\mathrm{j}}} + w_i c) = 0 \ in\ \Omega_F \qquad [21]$$

where the boundary conditions are:

$$(a_{\mathrm{ijkl}}\, e_{\mathrm{kl}}(\boldsymbol{u}) + p\delta_{ij} - \varepsilon\,\mu_F (w_{i,j} + w_{j,i}))N_j = 0 \ on\ \Gamma \qquad [22]$$

$$w_{\mathrm{i}} = 0 \ on\ \Gamma \qquad [23]$$

$$(-D_{ij} \frac{\partial c}{\partial X_{\mathrm{j}}})N_i = 0 \ on\ \Gamma \qquad [24]$$

and the periodicity conditions of all unknowns holds.

3.2 Asymptotic developments method.

In the homogenization process the unknowns (i.e. solid displacement, fluid velocity and fluid pressure) are presented in the form of asymptotic developments (([SAN 80, BEN 78]).

$$u_i(\boldsymbol{x},\boldsymbol{y},t) = u_i^{(0)}(\boldsymbol{x},\boldsymbol{y},t) + \varepsilon\, u_i^{(1)}(\boldsymbol{x},\boldsymbol{y},t) + \varepsilon^2\, u_i^{(2)}(\boldsymbol{x},\boldsymbol{y},t) + ... \qquad [25]$$

$$p(\boldsymbol{x},\boldsymbol{y},t) = p^{(0)}(\boldsymbol{x},\boldsymbol{y},t) + \varepsilon\, p^{(1)}(\boldsymbol{x},\boldsymbol{y},t) + \varepsilon^2\, p^{(2)}(\boldsymbol{x},\boldsymbol{y},t) + ... \qquad [26]$$

$$w_i(\boldsymbol{x},\boldsymbol{y},t) = w_i^{(0)}(\boldsymbol{x},\boldsymbol{y},t) + \varepsilon\, w_i^{(1)}(\boldsymbol{x},\boldsymbol{y},t) + \varepsilon^2\, w_i^{(2)}(\boldsymbol{x},\boldsymbol{y},t) + ... \qquad [27]$$

Each term in the asymptotic development is assumed periodic which means that it takes the same values in the corresponding points at the opposite walls of the period. Because of the existence of two separate scales the derivation operator in [18]-[24] is transformed into $\frac{\partial}{\partial \boldsymbol{y}} \rightarrow \frac{\partial}{\partial \boldsymbol{y}} + \varepsilon \frac{\partial}{\partial \boldsymbol{x}}$. Note that we have

$$e_{xij}(\boldsymbol{u}) = \frac{1}{2}(\frac{\partial u_{\mathrm{i}}}{\partial x_j} + \frac{\partial u_{\mathrm{j}}}{\partial x_i}) \ \text{and} \ e_{yij}(\boldsymbol{u}) = \frac{1}{2}(\frac{\partial u_{\mathrm{i}}}{\partial y_j} + \frac{\partial u_{\mathrm{j}}}{\partial y_i}).$$

In the process of homogenization the asymptotic developments [25]-[27] are introduced in the microscopic description [18]-[24], while simultaneously applying the two scale derivation operator. After identification of all terms staying by the same powers of ε, we obtain a series of successive order problems to be solved in the period. Typically, the first problem gives the solution for the term of the order zero (for example in case of displacement: the form of $\boldsymbol{u}^{(0)}(\boldsymbol{x},\boldsymbol{y},t)$). From the second problem we obtain the solution for the term of the order one

(for example in case of displacement: the form of $\boldsymbol{u}^{(1)}(\boldsymbol{x},\boldsymbol{y},t)$) that means the first corrector. Finally, the third problem is subjected to volume averaging in order to obtain the macroscopic description (model).

In section 3.3 the solutions of the homogenization process are presented. For more details concerning the homogenization of the problem [18]-[20] with the conditions [22]-[23] (see [AUR 77]). For the problem [21] and [24], see [AUR 96].

3.3 Solutions

3.3.1 The zero-order solutions

The analysis starts with the solution for the leading order of the main variables: $p^{(0)}$, $u^{(0)}$ and $c^{(0)}$.

The first problem is for pressure $p^{(0)}$ and comes from [19]:

$$\frac{\partial p^{(0)}}{\partial y_i} = 0 \ in \ \Omega_F \qquad [28]$$

where $p^{(0)}$ is periodic. The solution to this problem is $p^{(0)}(\boldsymbol{x},\boldsymbol{y},t) = p^{(0)}(\boldsymbol{x},t)$.

The second problem defines the displacement $u^{(0)}$ and comes from [18] and [22]:

$$\frac{\partial}{\partial y_j}(a_{ijkl}\, e_{ykl}(\boldsymbol{u}^{(0)})) = 0 \ in \ \Omega_S \qquad [29]$$

$$(a_{\mathrm{ijkl}}\, e_{\mathrm{kl}}(\boldsymbol{u}^{(0)}))N_j = 0 \ on \ \Gamma \qquad [30]$$

where $\boldsymbol{u}^{(0)}$ is periodic. The solution is $u^{(0)}(\boldsymbol{x},\boldsymbol{y},t) = u^{(0)}(\boldsymbol{x},t)$.

The third problem is for $c^{(0)}$ and is given by [21] and [24]

$$\frac{\partial}{\partial y_{\mathrm{i}}}(-D_{ij}\frac{\partial c^{(0)}}{\partial y_{\mathrm{j}}}) = 0 \ in \ \Omega_F \qquad [31]$$

$$(-D_{ij}\frac{\partial c^{(0)}}{\partial X_{\mathrm{j}}})N_i = 0 \ on \ \Gamma \qquad [32]$$

where $c^{(0)}$ is periodic. The solution is $c^{(0)}(\boldsymbol{x},\boldsymbol{y},t) = c^{(0)}(\boldsymbol{x},t)$.

We can see that for each physical phenomenon we defined a macroscopic variable which does not depend on the microscopic space variable y.

The analysis is continued at the next order for the problem [19], [20] and [23], to obtain a solution for the relative flow velocity $\boldsymbol{w}^{(0)}(\boldsymbol{x},\boldsymbol{y})$:

$$\mu_F \frac{\partial^2 w_i^{(0)}}{\partial y_j \partial y_j} - \frac{\partial p^{(1)}}{\partial y_i} - \frac{\partial p^{(0)}}{\partial y_i} = 0 \ in \ \Omega_F \quad [33]$$

$$\frac{\partial w_i^{(0)}}{\partial y_i} = 0 \ in \ \Omega_F \quad [34]$$

$$w_i^{(0)} = 0 \ on \ \Gamma \quad [35]$$

where $p^{(1)}$ and $w_i^{(0)}$ are periodic. The solution to the problem [33]-[35] is

$$w_i^{(0)} = - \mathrm{k_{ij}} \frac{\partial p^{(0)}}{\partial x_j} \quad [36]$$

If we substitute $w_i^{(0)}$ according to $w_i = v_i - \dot{u}_i$, and calculate the volume average of the relative velocity, we obtain the Darcy law in the form ([AUR 77])

$$< w_i^{(0)} > = < v_i^{(0)} > - n \dot{u}_i = - K_{\mathrm{ij}} \frac{\partial p^{(0)}}{\partial x_j} \quad [37]$$

where $K_{ij} = < k_{ij} >$ is the macroscopic permeability tensor. It can be computed from the local boundary value problem that arises, after injection of [36] into [33]- [35] ([AUR 05, AUR 77]).

3.3.2 The first-order solutions

The next problem concerning the solid behaviour comes from [18] and [22] and defines $u_i^{(1)}$

$$\frac{\partial}{\partial y_j} (a_{ijkl} \ (e_{ykl}(\boldsymbol{u}^{(1)}) + e_{xkl}(\boldsymbol{u}^{(0)}))) = 0 \ in \ \Omega_S \quad [38]$$

$$(a_{\mathrm{ijkl}} \ (e_{ykl}(\boldsymbol{u}^{(1)}) + e_{xkl}(\boldsymbol{u}^{(0)})))N_j = - p^{(0)} N_i \ \ on \ \Gamma \quad [39]$$

where $u_i^{(1)}$ is periodic. The solution is a linear function as follows

$$u_i^{(1)} = \xi_i^{kl} e_{xkl}(\boldsymbol{u}^{(0)}) - \eta_{\mathrm{i}} \ p^{(0)} + \bar{u}_i^{(1)}(\boldsymbol{x}, t) \quad [40]$$

where $\bar{u}_i^{(1)}(\boldsymbol{x}, t)$ is an arbitrary vector. The characteristic (microscopic) functions $\boldsymbol{\xi}$ and $\boldsymbol{\eta}$ are a third order tensor and a vector, respectively. They can be computed from the local boundary problem if we inject [40] into [38] and [39] ([AUR 77, ENE 84]).

The next order approximation of the concentration, $c^{(1)}$ is the solution of a problem obtained from [21] and [24]:

$$- \frac{\partial}{\partial y_i} (D_{ij} (\frac{\partial x^{(1)}}{\partial y_j} + \frac{\partial x^{(0)}}{\partial x_j})) = 0 \ in \ \Omega_F \quad [41]$$

$$-(D_{ij}(\frac{\partial c^{(1)}}{\partial y_j}+\frac{\partial c^{(0)}}{\partial x_j}))N_i = 0 \; on \; \Gamma \qquad [42]$$

where $c^{(1)}$ is periodic. In [41]- [42] we took into account that $c^{(0)}(\boldsymbol{x},t)$. The solution is a linear function of the macroscopic gradient of concentration

$$c^{(1)} = \zeta_i \frac{\partial c^{(0)}}{\partial x_i} + \bar{c}^{(1)}(\boldsymbol{x},t) \qquad [43]$$

where $\bar{c}^{(1)}(\boldsymbol{x},t)$ is an arbitrary function. The characteristic vectorial function $\boldsymbol{\zeta}$ can be calculated, if we introduce the solution [43] into the problem [41]-[42]. For details see [AUR 96].

3.3.3 The macroscopic equations

From [18], [19] and [22] at the next order we obtain the following set of equations

$$\frac{\partial \sigma_{Sij}^{(1)}}{\partial y_j}+\frac{\partial \sigma_{Sij}^{(0)}}{\partial x_j} = 0 \; in \; \Omega_S \qquad [44]$$

$$\frac{\partial \sigma_{Fij}^{(1)}}{\partial y_j}-\frac{\partial p^{(0)}}{\partial x_i} = 0 \; in \; \Omega_F \qquad [45]$$

$$\sigma_{Sij}^{(1)} N_j = \sigma_{Fij}^{(1)} N_j \; on \; \Gamma \qquad [46]$$

with the periodicity conditions.

In order to obtain the macroscopic equations, equations [44] and [45] are integrated over the respective domains, and summed. Then, the boundary condition [46] is applied, that leads to the elimination of the derivatives with respect to the microscopic variable y. Finally, the macroscopic equilibrium equation is get [AUR 77]

$$< \frac{\partial \sigma_{ij}^{T(0)}}{\partial x_j} > = 0 \qquad [47]$$

where $\sigma^{T(0)}$ is the total stress tensor that is written as $\sigma^{(0)}_S$ and $\sigma^{(0)}_F$ within the respective domains Ω_S and Ω_F . After several transformations consisting mainly in the introduction of the solution for $u_i^{(1)}$ in the expression for stresses in the solid domain we can write the total stress tensor in the form [AUR 77]

$$\sigma_{ij}^{T(0)} = C_{ijkl}\, e_{xkl}(u^{(0)}) - \alpha_{ij}\, p^{(0)} \qquad [48]$$

where

$$\sigma_{Sij}^{(0)} = C_{ijkl}\, e_{xkl}(u^{(0)}) \qquad [49]$$

and the macroscopic elasticity tensors C_{ijkl} and α_{ij} mean the rigidity tensor and the hydro-mechanical coupling elasticity tensor, respectively [AUR 77]

$$C_{ijkl} = < a_{ijkl} + a_{ijmn}\ e_{ymn}(\xi^{kl}) > \quad [50]$$

$$\alpha_{ij} = n\, I_{ij} + < a_{ijmn}\ e_{ymn}(\eta) > \quad [51]$$

Both tensors can be computed for a given microstructure of the period, after the solution of the local boundary problems for ξ and η.

The second macroscopic equation is obtained from equation [20]. At the order ε it gives

$$\frac{\partial w_i^{(0)}}{\partial x_i} + \frac{\partial w_i^{(1)}}{\partial y_i} = 0 \ in\ \Omega_F \quad [52]$$

Next, equation [52] is integrated within the domain Ω_F. We take into account the continuity of displacement on Γ, equation [23] and the previously obtained solution for $\boldsymbol{u}^{(0)}$. Finally, the following macroscopic equation is get [AUR 77]

$$\frac{\partial (< v_i^{(0)} > - n\, \dot{u}_i)}{\partial x_i} = - \gamma_{ij}\, \dot{e}_{xij}(\boldsymbol{u}^{(0)}) - \beta\, \dot{p}^{(0)} \quad [53]$$

where γ and β are two new coupling tensor and vector that are defined as follows:

$$\gamma_{ij} = n\, I_{ij} - < \xi_{p,p}^{ij} > \quad [54]$$

$$\beta = < \eta_{p,p} > \quad [55]$$

It can be shown that $\gamma = \alpha$ [AUR 77]

Concerning the transport of the dissolved CO_2, from [21] and [24] we have

$$\frac{\partial c^{(0)}}{\partial t} - \frac{\partial}{\partial x_i}(D_{ij}(\frac{\partial c^{(0)}}{\partial x_j} + \frac{\partial c^{(1)}}{\partial y_j})) - \frac{\partial}{\partial y_i}(D_{ij}(\frac{\partial c^{(1)}}{\partial x_j} + \frac{\partial c^{(2)}}{\partial y_j})) + \frac{\partial}{\partial x_i}(w_i^{(0)} c^{(0)}) + \frac{\partial}{\partial y_i}(w_i^{(1)} c^{(0)} + w_i^{(0)} c^{(1)}) = 0 \ in\ \Omega_F \quad [56]$$

$$-(D_{ij}(\frac{\partial c^{(1)}}{\partial x_j} + \frac{\partial c^{(2)}}{\partial y_j}))N_i = 0 \ on\ \Gamma \quad [57]$$

In order to obtain the macroscopic equation, eq. [56] is integrated over the volume Ω_F. Next, the interface condition [57], the periodicity, eq. [23] and the solution for $c^{(0)}$, are applied. After introduction of the solution [43] the final form of the macroscopic diffusion-convection equation is obtained ([AUR 96])

$$n\frac{\partial c^{(0)}}{\partial t} - \frac{\partial}{\partial x_i}(D_{ij}^{*}\frac{\partial c^{(0)}}{\partial x_j}) + \frac{\partial}{\partial x_i}(c^{(0)} < w_i^{(0)} >) = 0 \qquad [58]$$

where the macroscopic diffusion tensor D_{ij}^{*} is defined as

$$D_{ij}^{*} = \frac{1}{|\Omega|}\int_{\Omega_F}(D_{ik}(I_{kj} + \frac{\partial \zeta_j}{\partial y_k}))d\Omega \qquad [59]$$

and $< w_i^{(0)} >$ is the Darcy velocity.

3.4 Summary of the macroscopic "H-M-T model"

Let us summarize the results of homogenization performed in the section 3. The macroscopic model of coupled fluid flow, CO_2 transport and solid deformation ("H-M-T model") is defined by a set of macroscopic equations: [47]-[48], [53], [37] and [58]. The model shows two kinds of couplings that can be called: the "weak" and the "strong" coupling. The "weak" coupling can be observed between the fluid flow and the CO_2 transport, through the water velocity appearing in [58]. The "strong" coupling is the hydro-mechanical coupling that can be seen in [53] and [48].

The advantage of modelling by homogenization is that it provides the definitions of the macroscopic parameters, like the rigidity tensor $\boldsymbol{C}$ (see [50]), the hydro-mechanical coupling tensor $\boldsymbol{\alpha}$ ([51]) and the scalar β (see [55]), and the effective diffusion tensor $\boldsymbol{D}^*$ ([59]). All these quantities can be calculated, if the microstructure of the porous aquifer is known, by using numerical methods.

4. Homogenization of the C-M problem

Let us now assume that the porous medium is subjected to homogeneous solid dissolution. Such situation corresponds to the long-term (slow) degradation mechanism. In this section we focus on the analysis of the chemo-mechanical coupling. We are interested in the progressive alteration of the mechanical parameters as a consequence of material dissolution.

4.1 Formulation of the problem at the microscopic scale

The following two microscopic problems for the non-dimensional variables are formulated in the period domain (Figure 3):

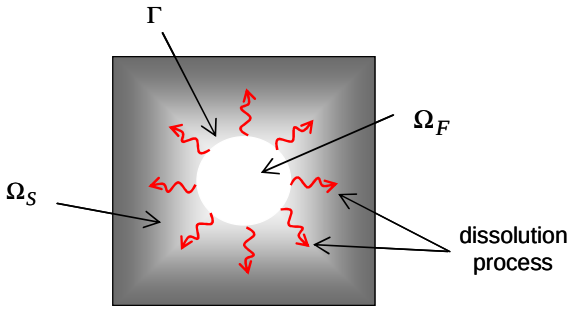

Figure 3. The dissolution of the solid in the period

- The mechanical “M-problem”:

We recall the previously formulated mechanical problem, with $a_{ijkl}(\boldsymbol{y})$ being now the microscopic rigidity tensor depending on the local space variable **y**

$$\sigma_{Sij,j} = 0 \ in \ \Omega_S \quad [60]$$

$$\sigma_{Sij} = a_{ijkl}\, e_{kl}(\boldsymbol{u}) \ in \ \Omega_S \quad [61]$$

$$e_{kl} = 1/2\,(u_{k,l} + u_{l,k})$$

$$\sigma_{Sij} N_j = 0 \ on \ \Gamma \quad [62]$$

- The chemical “C-problem”:

The dissolution problem is governed by a single diffusion equation for the concentration in solid (solid fraction) c_S , with one characteristic parameter D_S describing the rate of the process. Such assumption is an evident simplification of the complex chemical reactions taking place at the microscopic scale, and will be used as a first approach to the problem. We further introduce a local dissolution mechanism. This process starts at the interface Γ , and progresses towards the inside of the solid (Figure 3)

$$c_S(y,t) = 0 \ in \ \Omega_F \quad [63]$$

$$\frac{\partial c_S}{\partial t} = div(\boldsymbol{D}_S \ grad \ c_S) \ in \ \Omega_S \quad [64]$$

where the boundary and initial conditions are

$$c_S = 0 \ on \ \Gamma \quad [65]$$

$$N\,(D_S \ grad \ c_S) = 0 \ on \ \partial\Omega_S \cap \partial\Omega \quad [66]$$

$$c_S(t=0) = 1 \ in \ \Omega_S$$

where $\boldsymbol{D}_S$ is the diffusion tensor related to the evolution of the solid dissolution. Note that we further assume that it is constant but the extension to the case $D_S(c_S)$ is possible.

The dissolution problem is time-dependent which makes the associated elasticity problem also time-dependent, through the dependence of the local rigidity tensor a_{ijkl} on the concentration in solid (c_S). It is assumed that the constitutive relationship $a_{ijkl}(c_S)$ is known.

4.2 Homogenization

The homogenization process follows the classical scheme. It can be shown that the results obtained have similar form as those presented in section 3.3. In this case the macroscopic model is written:

$$< \frac{\partial \sigma_{Sij}^{(0)}}{\partial x_j} > = 0 \qquad [67]$$

where the macroscopic stress tensor is

$$\sigma_{Sij}^{(0)} = C_{ijkl}\, e_{xkl}(u^{(0)}) \qquad [68]$$

The macroscopic tensor C_{ijkl} is the rigidity tensor that can be obtained from the iterative solution of the local boundary value problem. The local boundary value problem is the same as in the case presented in section 3.3.2. It should be noted that in the case considered in this section we have to solve the coupled chemo-mechanical problem for each time increment. The two local boundary value problems to be solved simultaneously are:

- The mechanical "M-problem":

$$\frac{\partial}{\partial y_j}(a_{ijkl}(c_S) + a_{ijmn}(c_S)\, e_{ymn}(\xi^{kl})) = 0 \ in\ \Omega_S \qquad [69a]$$

$$(a_{ijkl}(c_S) + (a_{ijmn}(c_S)\, e_{ymn}(\xi^{kl}))N_j = 0 \ on\ \Gamma \qquad [69b]$$

ξ^{kl} is periodic [69c]

- The chemical "C-problem":

$$\frac{\partial c_S}{\partial t} = div(D\, grad\, c_S) \ in\ \Omega_S \qquad [70a]$$

$$c_S = 0 \ on\ \Gamma \qquad [70b]$$

$$N(D\, grad\, c_S) = 0 \ on\ \partial\Omega_S \cap \partial\Omega \qquad [70c]$$

$$c_S(t = 0) = 1 \ in\ \Omega_S \qquad [70d]$$

The unknown of the problem is the displacement vector $\xi^{kl}(\xi_1^{kl}, \xi_2^{kl}, \xi_3^{kl})$ which depends on the local space variable y and time t, $\xi^{kl}(y,t)$. Remark that ξ^{kl} is a particular periodic solution corresponding to the unit macroscopic strain tensor $\mathbf{E}^{kl} = (e_k \otimes e_l + e_l \otimes e_k)/2$. where k, l = 1, 2, 3. The symbol ⊗ means the tensorial product between the unit vectors of the basis. This solution should also verify the zero volume average condition.

Once ξ^{kl} is known, the macroscopic rigidity tensor is defined as the volume average for each time increment as follows:

$$C_{ijkl} = < a_{ijkl}(c_S) + a_{ijmn}(c_S)\, e_{ymn}(\xi^{kl}) > \qquad [71]$$

Thus, the macroscopic tensor is time-dependent, $\boldsymbol{C}(t)$. In section 5 we present an example of the numerical computations of this tensor for a particular microstructure of the porous medium.

4.3 Summary of the macroscopic "C-M model"

The chemo-mechanical model related to the modification of the microstructure of the porous aquifer, is proposed. The model consists of the macroscopic equation of the mechanical equilibrium [67]-[68] that is coupled with the local model describing the chemical degradation of the mechanical parameters ([69]-[70]-[71]). The computations of the evolution of the mechanical parameters can be carried out, if the initial microstructure is given.

It has to be pointed out that the presented model does not take into account the modification of the hydro-mechanical coupling parameters (as proposed in [LEW 12]).

5. Numerical computations of the time degradation of the macroscopic rigidity tensor.

5.1 Definition of the problem.

Let us analyse the porous medium presenting three dimensional periodic microstructure, Figure 4. The period is a cube of the unit dimension. The three cylinders representing pores have the diameter 0.1. Both domains (fluid Ω_F and solid Ω_S) are connected. The aim is to calculate the macroscopic fourth order rigidity tensor that can be converted into the second order tensor (6×6) by using the classical conversion rules. The two coupled chemo-mechanical problems (69)-(70) were solved using the commercial code Comsol Multiphysics.

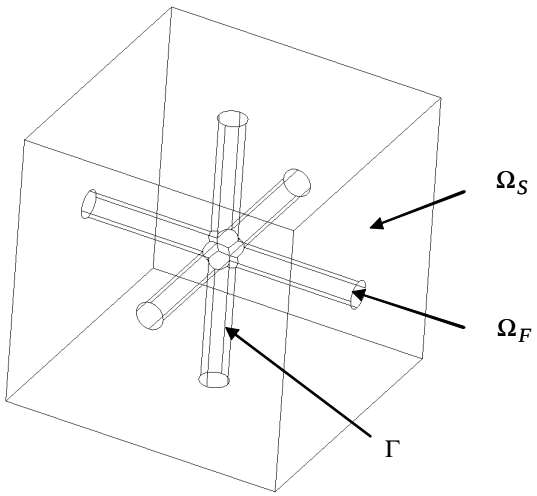

Figure 4. The microstructure considered in the numerical example

Initially, the (intact) material is locally isotropic with two elasticity parameters: the Young modulus E=1 and the Poisson ratio ν=0.2. As a first approximation it is assumed that the local constitutive relationship $a_{ijkl}(c_S)$ is such that the only parameter affected by the local variation of the volumetric fraction of the solid is the Young modulus. We used the formula of

Hashin and Shtrikman (1963) for the upper bound of the effective Young modulus of a porous material [ROB 02] :

$$\frac{E}{E_S} = \frac{c_S}{1 + S(1 - c_S)} \qquad [62]$$

where S is given as a function of the Poisson ratio ν_S by the following formula

$$S = \frac{(1 + \nu_S) \times (13 - 15\nu_S)}{2 \times (7 - 5\nu_S)} \qquad [63]$$

and c_S is the solid fraction. In the example the tensor $\boldsymbol{D}_S$ is assumed isotropic $\boldsymbol{D}_S = D_S \boldsymbol{I}$, where $\boldsymbol{I}$ is the identity matrix and $D_S = 10^{-9} m^2 / s$.

The period possesses three identical planes of geometry and material symmetry, therefore the rigidity tensor at the macroscopic scale presents cubic symmetry, with three independent elasticity parameters. The following general property holds: $D_{11}=D_{22}= D_{33,}$ $D_{12}=D_{13}= D_{23} =D_{21}= D_{31} =D_{32,}$ $D_{44}=D_{55}= D_{66}$ In order to calculate the components D_{11}, D_{21}, and D_{66}, two elementary mechanical problems have to be solved, namely the traction test and the shearing test. We considered the tests:

- traction test with $\mathbf{E}^{11} = (e_1 \otimes e_1 + e_1 \otimes e_1)/2$.
- shearing test with $\mathbf{E}^{12} = (e_1 \otimes e_2 + e_1 \otimes e_2)/2$.

For each test we take into account the transient chemical degradation of the local parameters of the material.

Because of the symmetry, instead of solving the coupled problem (69)-(70) in the full period domain with the periodicity conditions, we solved the problem in the 1/8 of the period (the volume is $0.5 \times 0.5 \times .0.5$) with the appropriate boundary conditions as in [BOR 01]. For example, for the traction tests the boundary conditions on all external boundaries are:

$u_N = 0$ and $\sigma_T = 0$.

For the shearing test in the plane (i, j) we have the following conditions:

$u_T = 0$ and $\sigma_N = 0$ on the external boundaries orthogonal to the axis i and j,

$u_N = 0$ and $\sigma_T = 0$ on the external boundaries orthogonal to the axis k.

where u_N and u_T are the displacement in the direction normal to the plane and the displacement in the directions tangent to the plane, respectively. σ_N and σ_T are the normal and tangential stress components.

5.2 Results and discussion

In Figure 5a the result of the computations of the solid concentration (solid fraction) at time t = 1e7 is presented. We can observe the decrease of the solid concentration initiated in the pores. The maximum value in the domain is equal 1. In Figure 5b the intensity of the displacement vector $\boldsymbol{\xi}^{11}(\xi_1^{11}, \xi_2^{11}, \xi_3^{11})$ at t= 1e7 for the case of unit macroscopic traction test in the direction 1, is shown. In Figures 6a and 6b the solid concentration and the intensity of

the displacement vector ξ^{11} at t= 1e8 are presented. The maximum value of the concentration in the domain at this time is equal to 0.594. It can be observed that strain is localized in the weak (the most altered) zones.

In Figure 7 the three components of the rigidity tensor, C_{11}, C_{12} and C_{66}, as functions of time and as function of average matrix porosity, are plotted. It can be seen that all components of the rigidity matrix are logarithmically decreasing with time. On the other hand, a dramatic decrease of all three components with the increasing average porosity (or decreasing average solid concentration) of the matrix is seen. If we interpret the results in terms of engineering parameters (Figure 8), we can see that the Poisson ratio ν seems to decrease to an asymptotic value equal to 90% of the initial value. Note that it was assumed that the local Poisson ratio in not altered. The Young modulus E and the shear modulus G decrease significantly to about 50% of the initial values for the average porosity of the matrix of approximately 30%. The most affected parameter in this case is the shear modulus.

The results of numerical computations using the model obtained by homogenization can be compared with the experiments published in the literature (e.g. [NGU 11]). For example, in Figure 9 [NGU 11] the drained bulk modulus and the shear modulus against porosity for the carbonate samples (named by the authors the Euville limestone), are plotted. These parameters were measured in standard triaxial tests. The curves show a decrease of the parameters under the effect of chemical alteration, which manifests itself by the increase of the porosity. It can be seen that these curves agree qualitatively with the computed curves, coming from coupled chemo-mechanical model obtained by homogenization. It has to be pointed out that the microstructure of the carbonate investigated in [NGU 11] is very complex, with bimodal distribution of pore sizes (microporosity and macroporosity). It is believed that the quantitative reproduction of the observed behaviour would be possible by following the presented approach, if the real geometry of the microstructure would be considered.

6. Conclusions

The macroscopic models describing the behaviour of a porous saturated aquifer in which the injected CO_2 is migrating, are presented. The theoretical framework is the homogenization of periodic structures. This homogenization method is one of the micromechanical approaches that are very well established in the literature. The analysis was focused on the long term effects, including the chemo-mechanical coupling. The model of chemical degradation and mechanical weakening of the material at long time was proposed. It was shown that the chemo-mechanical coupled computations for a particular three dimensional microstructure can be performed by using the finite elements commercial code Comsol Multiphysics.

The results of the numerical computations of the full macroscopic rigidity tensor showed the degradation with time of all non-zero components of the tensor. Also, the decrease of the rigidity tensor is observed with the decrease of the average solid fraction (or increase of the average porosity). The material of porous aquifer analysed in the numerical example shows the cubic symmetry at the macroscopic scale (cubic anisotropy). The three (independent) engineering elasticity parameters (E, G and ν) decrease with time. It can be seen that the proposed degradation mechanism leads to the significant decrease of the Young modulus and the shear modulus when the average porosity increases from 0 to 30 %, while at the same time the Poisson ratio seems to tend to as asymptotic value of 90% of the initial value.

The comparison between the numerical computations and the experimental data published in the literature showed that the proposed model of chemo-mechanical coupling is able to qualitatively reproduce the curves of the elastic parameters of a rock subjected to the chemical alteration. In order to enable the quantitative comparison, the computations have to be performed for the real geometry of the microstructure.

Further investigations concerning the chemical modification of the microstructure and its geomechanical effects are currently carried out.

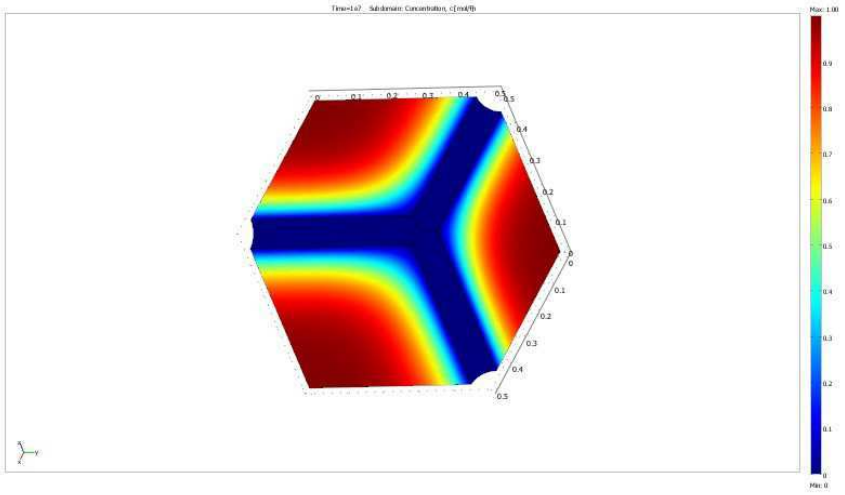

Figure 5a. The distribution of the solid concentration from 0 to 1 in the 1/8 of the period at time $t=10^7$s

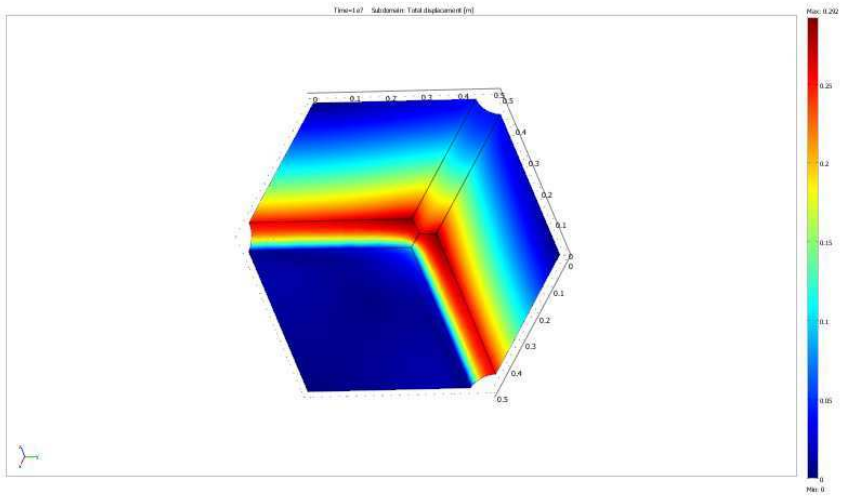

Figure 5b. The intensity of the displacement vector $\boldsymbol{\xi}^{11}$ $(\xi_1^{11}, \xi_2^{11}, \xi_3^{11})$ in the 1/8 of the period at time $t=10^7$s. The axis 1 is orthogonal to the surface seen in the frontal plane.

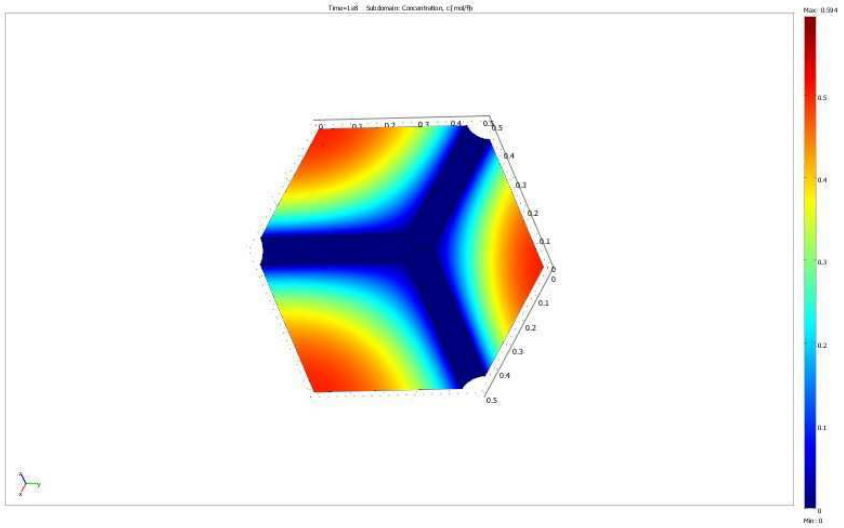

Figure 6a. The distribution of the solid concentration from 0 to 0.594 in the 1/8 of the period at time t=10^8s

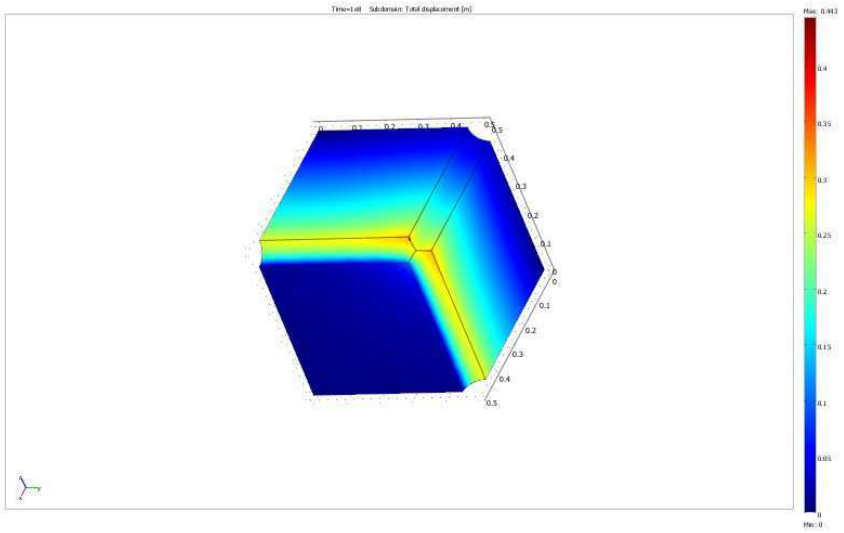

Figure 6b. The intensity of the displacement vector $\boldsymbol{\xi}^{11}(\xi_1^{11}, \xi_2^{11}, \xi_3^{11})$ in the 1/8 of the period at time t=10^8s. The axis 1 is orthogonal to the surface seen in the frontal plane.

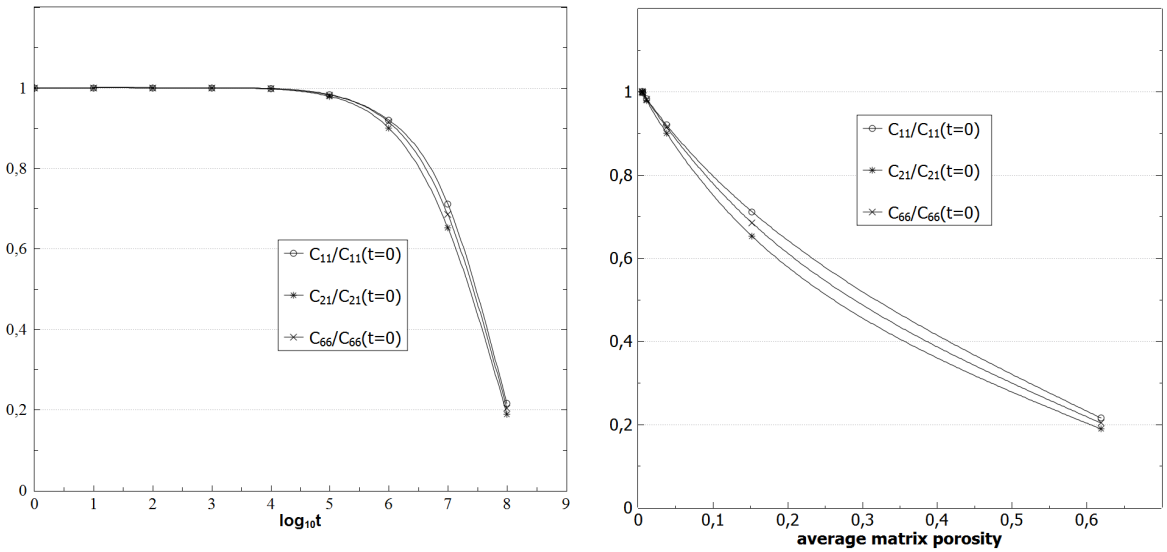

a) b)

Figure 7. The plots of the three components of the macroscopic rigidity tensor: C_{11}, C_{12} and C_{66}, as functions of time (a), and as functions of the average matrix porosity (b).

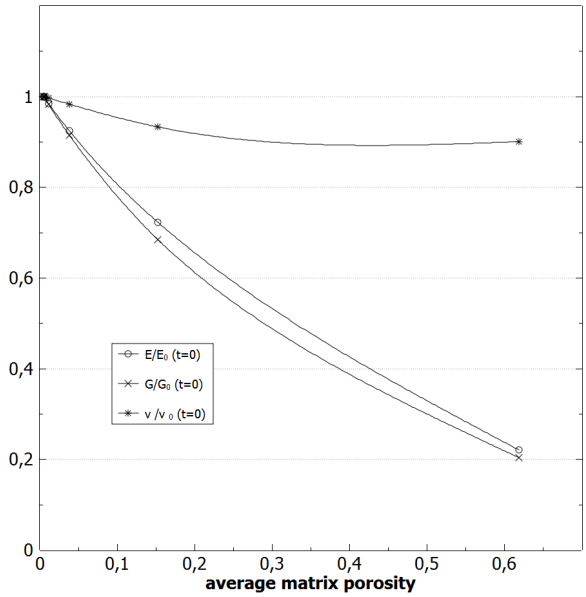

Figure 8. The variation of the three independent engineering parameters of elasticity (E, G, ν) with respect to the initial values (at t=0) as a function of the average matrix porosity.

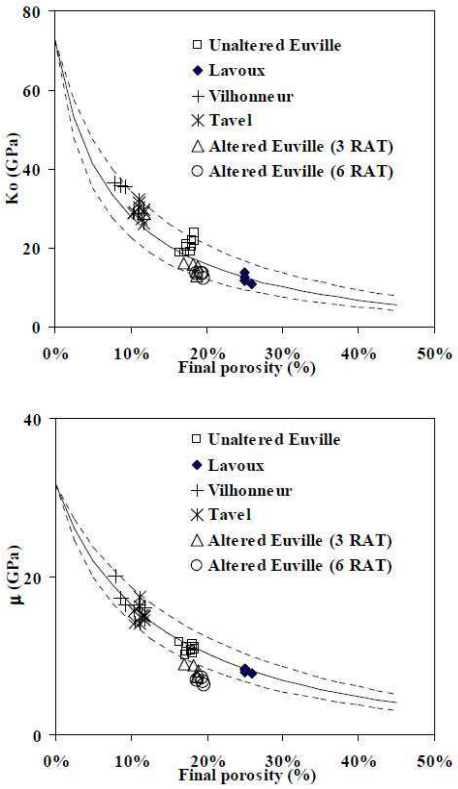

Figure 9. The experimental data of the degradation of the elastic parameters (K, G) of limestone rocks when subjected to chemical alteration.
Reproduced after [NGU 11] (permission has been requested).

Acknowledgement:

The numerical computations were performed by Artur Lipkowski (Gdansk University of Technology, Poland) in the framework of his Master thesis prepared at the University of Montpellier 2, Laboratory LMGC (ERASMUS 2012).

Bibliography:

[AUR 91] AURIAULT J.-L., "Heterogeneous medium. Is an equivalent description possible?" *Int. Journal Engng. Sci.*, vol. 29, No 7, pp. 785-795, 1991.

[AUR 96] AURIAULT J.-L., LEWANDOWSKA J., "Diffusion/adsorption/advection macrotransport in soils", *Eur. J. Mech. A/Solids*, 15, No 4, pp. 681-704, 1996.

[AUR 05] AURIAULT J.-L., "Upscaling by multiscale asymptotic expansions". In: CISM Lecture 480 *Applied micromechanics of porous materials*. Udine 19-23 July 2004. L. Dormieux and F.-J. Ulm Eds Springer pp. 3-56, 2005

[AUR 77] AURIAULT J.-L., SANCHEZ-PALENCIA E. "Etude du comportement macroscopique d'un milieu poreux saturé déformable", *Journal de Mécanique*, Vol. 16, No 4, 1977.

[BEN 78] BENSSOUSSAN A., LIONS J.L., PAPANICOLAOU G., *Asymptotic Analysis for Periodic Structures*, North-Holland, Amsterdam, Netherlands, 1978.

[BER 09] BERNER E., LOMBARD J., "From Injectivity to Integrity Studies of CO2 Geological Storage Chemical Alteration Effects on Carbonates". *Oil & Gas Science and Technology*, 2009, Rev. IFP DOI: 10.2516/ogst/2009028.

[BOR 11] BORNERT M., BRETHEAU T., GILORMINI P. (Edts) *Homogénéisation en mécanique des matériaux 1*. HERMES Science Europe Ltd, Paris, 2011.

[EGE 05] EGERMANN P., BEKRI S., VIZIKA O. "An Integrated Approach to Assess the Petrophysical Propertes of Rocks Altered by Rock/Fluid Interactions (CO2 injection) ". Paper SCA presented at the Society of Core Analysts Symposium, Toronto, Canada, August 21-25, 2005.

[ENE 84] ENE F., *Contribution à l'étude des matériaux composites et leur endommagement*. Thèse de Doctorat d'Etat Sciences Mathématiques (Mécanique). Université Pierre et Marie Cuire Paris VI, 1984.

[GOU 10] GOUZE P., LUQUOT L., "X-ray microtomography characterization of porosity, permeability and reactive surface changes during dissolution", *J. Contam. Hydrol.*, 2010, doi:10.1016/j,jconhyd.2010.07.004

[IZG 08] IZGEC O., DEMITRAL B., BERTIN H., AKIN S.,"CO2 injection into saline carbonate aquifer formations I: laboratory investigation". *Transport in Porous Media*, 72, 1, pp. 1-24, 2008.

[LEW 12] LEWANDOWSKA J., AURIAULT J.-L., *"Extension of Biot theory to the problem of saturated microporous elastic media with isolated cracks or/and vugs". International Journal for Numerical and Analytical Methods in Geomechanics. 2012, DOI: 10.1002/nag.2150.*

[LUQ 09] LUQUOT L., GOUZE P., "Experimental determination of porosity and permeability changes induced by injection of C02 into carbonate rocks". *Chemical Geology*, 265, 3, pp. 148-159, 2009.

[NGU 11] NGUYEN M. T. *Caractérisation géomécanique de la degradation des roches sous l'effet de l'injection de gaz acides*. PhD thesis, University Paris-Est, 2012.

[NGU 11] NGUYEN M. T., BERNER M. T., DORMIEUX L., *"Micromechanical modeling of carbonate geomechanical properties evolution during acid gas injection"*. The 45th US Rock Mechanics/ Geomechanics Symposium, San Francisco, CA, June 26-29, 2011. ARMA, American Rock Mechanics Association, 10 pages, 2011.

[ROB 02] ROBERTS P., GARBOCZI E. J., "Computation of the linear elastic properties of random porous material with wide variety of microstructure". *Proc. R. Soc. Lond. A*, 458, pp. 1033-1054, 2002, doi:10.1098/rspa.2001.0900

[SAN 80] SANCHEZ-PALENCIA E, *Non-Homogeneous Media and Vibration Theory*, Berlin Heidelberg New York, Springer – Verlag, 1980.